# A Hybrid Brain Computer Interface to Control the Direction and Speed of a Simulated or Real Wheelchair

**Article** *in* IEEE transactions on neural systems and rehabilitation engineering: a publication of the IEEE Engineering in Medicine and Biology Society · June 2012

DOI: 10.1109/TNSRE.2012.2197221 · Source: PubMed



**6 authors**, including:

Hongtao Wang
Wuyi University
**60** PUBLICATIONS **1,354** CITATIONS

SEE PROFILE

Tianyou Yu
South China University of Technology
**20** PUBLICATIONS **533** CITATIONS

SEE PROFILE

Jiahui Pan
South China Normal University
**108** PUBLICATIONS **2,810** CITATIONS

SEE PROFILE

# A Hybrid Brain Computer Interface to Control the Direction and Speed of a Simulated or Real Wheelchair

Jinyi Long, Yuanqing Li, Hongtao Wang, Tianyou Yu, Jiahui Pan, and Feng Li

***Abstract*—Brain–computer interfaces (BCIs) are used to translate brain activity signals into control signals for external devices. Currently, it is difficult for BCI systems to provide the multiple independent control signals necessary for the multi-degree continuous control of a wheelchair. In this paper, we address this challenge by introducing a hybrid BCI that uses the motor imagery-based mu rhythm and the P300 potential to control a brain-actuated simulated or real wheelchair. The objective of the hybrid BCI is to provide a greater number of commands with increased accuracy to the BCI user. Our paradigm allows the user to control the direction (left or right turn) of the simulated or real wheelchair using left- or right-hand imagery. Furthermore, a hybrid manner can be used to control speed. To decelerate, the user imagines foot movement while ignoring the flashing buttons on the graphical user interface (GUI). If the user wishes to accelerate, then he/she pays attention to a specific flashing button without performing any motor imagery. Two experiments were conducted to assess the BCI control; both a simulated wheelchair in a virtual environment and a real wheelchair were tested. Subjects steered both the simulated and real wheelchairs effectively by controlling the direction and speed with our hybrid BCI system. Data analysis validated the use of our hybrid BCI system to control the direction and speed of a wheelchair.**

***Index Terms*—Direction, hybrid brain–computer interface (BCI), motor imagery, P300, speed, wheelchair.**

## I. Introduction

ELECTROENCEPHALOGRAM (EEG)-based brain-computer interfaces (BCIs) have attracted a great deal of attention because they are noninvasive, relatively convenient, and affordable [1]–[5]. One important application of EEG-based BCIs is wheelchair control, which can improve the quality of life and increase the independence of a disabled user [1], [3], [4]. The EEG signals used for wheelchair control include the P300 potential [6], steady-state visual evoked potentials (SSVEPs) [7], [8], and event-related desynchronization/synchronization (ERD/ERS) produced by motor imagery [9]. Until now, two types of protocols, synchronous and asynchronous, have been used for EEG-based wheelchair control. The EEG signals used for synchronous control depend on the potentials evoked by visual stimuli, including the P300 potential [2], [3] and the SSVEP [10]. Specifically, the location of a target is first selected using a P300- or SSVEP-based BCI [2], [3], and then, the wheelchair reaches the destination automatically by following a prepreprogrammed path [3] or by using a navigation system that avoids obstacles detected by an array of sensors [2]. The use of this synchronous protocol does not allow the user to change the direction or route of the wheelchair as it moves to its destination. These synchronous protocols exhibit high accuracy but suffer from a low response speed; an effective control command is generally achieved after several (e.g., 4) seconds [3].

The brain signals used for asynchronous control protocols are generally derived from motor imagery, allowing the user to send an appropriate command (e.g., a change in direction) to a moving wheelchair or object [4], [11], [12]. In a report by Galán *et al.* [4], directional control commands can be provided to a wheelchair by the evaluation of the ongoing EEG signals. These control commands depend on the user's mental activities (e.g., motor imagery).

Multi-degree control is essential to operate a wheelchair. For instance, several control signals are required to control the direction (left and right) and speed (acceleration and deceleration) as well as to start and stop the motion. Furthermore, these control commands must be accurately and quickly generated. Multiple independent control signals based on BCIs have been discussed in several studies [13]–[17]. McFarland *et al.* presented a BCI system that modulates various EEG rhythms, allowing continuous three-dimensional (3-D) cursor movement control [14]. In [16] and [17], BCI systems were used to control a virtual helicopter in 3-D space; motor imagery events including imagery of the left-hand, right-hand, tongue, foot and both hands, and the resting state generated several commands. A common characteristic of these BCI systems is the generation of control signals from a single modality of motor imagery.

Hybrid BCIs that can combine different brain signals are appealing regarding their ability to simultaneously or sequentially

Manuscript received November 23, 2011; revised March 18, 2012; accepted April 18, 2012. Date of publication June 06, 2012; date of current version September 07, 2012. This work was supported by National Natural Science Foundation of China under Grants 60825306, 91120305, and 60973113, by the National High-Tech R&D Program of China (863 Program) under Grant 2012AA011601, and by University High Level Talent Program of Guangdong Province, China. *Asterisk indicates corresponding author.*

J. Long, *Y. Li, and T. Yu are with the School of Automation Science and Engineering, South China University of Technology, Guangzhou 510640, China (e-mail: long.jinyi@mail.scut.edu.cn; auyqli@scut.edu.cn; yuty2009@gmail.com).

H. Wang is with the School of Information Engineering, WuYi University, Guangdong 529020, China.

J. Pan is with the School of Nanhai, South China Normal University, Foshan, Guangdong 528225, China.

F. Li is with the School of Computer and Communication Engineering, Changsha University of Science and Technology, Changsha 410114, China.

Color versions of one or more of the figures in this paper are available online at http://ieeexplore.ieee.org.

Digital Object Identifier 10.1109/TNSRE.2012.2197221

provide multiple control commands [18]–[22]. For example, Allison *et al.* demonstrated that combining multiple brain signals, such as motor imagery and SSVEP, can improve the accuracy of BCIs, especially that of the BCIs used by blind subjects [20], [23]. In our previous study [21], we presented a hybrid BCI that incorporates ERD/ERS and the P300 potential for continuous 2-D cursor control. Specifically, the horizontal and vertical cursor movements are separately and simultaneously controlled by motor imagery and the P300 potential, respectively. This system offers two advantages. First, there are two independent control signals generated from the type of motor imagery and the P300 potential. Second, the user can move the cursor from an arbitrary position to a randomly given target position. In [22], a hybrid task-based approach that combined motor imagery and the P300 potential into a single hybrid feature was proposed for target selection.

This paper proposes a hybrid BCI paradigm to provide directional and speed control commands to a simulated or real wheelchair. The control of the wheelchair speed is useful to the disabled. Generally, a real wheelchair provides several (e.g., 5) gear speeds. For instance, when the wheelchair is moving in the correct direction and there is a large distance between the wheelchair and the destination, it is better for the user to choose a middle or high speed. By contrast, it is better to choose a low speed when the wheelchair is making a sharp turn or moving along a narrow road. In our system, the left and right direction commands are based on the user's left- and right-hand imagery, respectively. Furthermore, a hybrid paradigm is used to control speed. To decelerate, the user imagines a third motor event (e.g., movement of the foot) while ignoring any flashing buttons on the graphical user interface (GUI). If the user wishes to accelerate, then he/she pays attention to a specific flashing button without imagining any movement. The flashing buttons on the GUI are set to evoke P300 potentials. Two experiments were conducted in this study. First, a simulated wheelchair was driven in a virtual environment to assess the performance of our proposed hybrid BCI. Second, a real wheelchair was driven using our hybrid BCI. Our experimental results and data analysis demonstrated the efficiency of our method.

This paper is organized into five sections. The methodologies, including the data acquisition system, GUI, control mechanism, models, and algorithms, are presented in Section II. Experimental results are described in Section III. Further discussion is given in Section IV. Section V concludes the paper.

## II. Methods

### A. EEG Data Acquisition

A NuAmps device (Compumedics) is used to measure scalp EEG signals for data acquisition. Each user wears an EEG cap (LT 37) that measures the signals from the electrodes shown in Fig. 1. The EEG signals are referenced to the right ear. Two channels, "HEOG" and "VEOG", representing eye movements are excluded (and not shown here). The EEG used for processing is recorded from Ag-AgCl electrodes that are placed at the sites in the frontal, central, parietal and occipital regions. The following 15 channels are included: "FC3," "FCz," "FC4," "C3," "Cz," "C4," "CP3," "CPz," "CP4," "P3," "Pz," "P4," "O1," "Oz," and "O2." Fig. 1 shows the locations of each site. All impedances are kept below 5 kΩ. The EEG signals are amplified, sampled at 250 Hz, and band-pass filtered between 0.5 and 100 Hz.

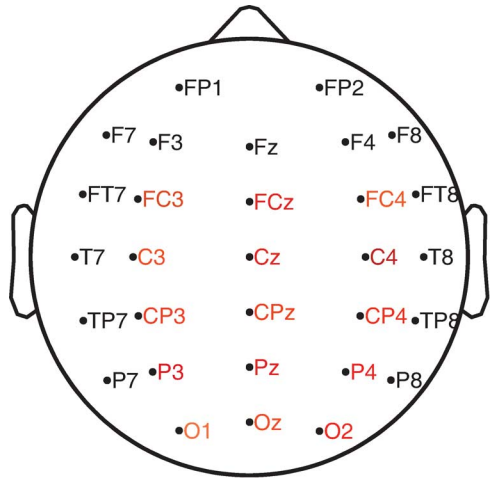


Fig. 1. Names and distribution of EEG cap electrodes. Fifteen channels (red color) are used for data processing.

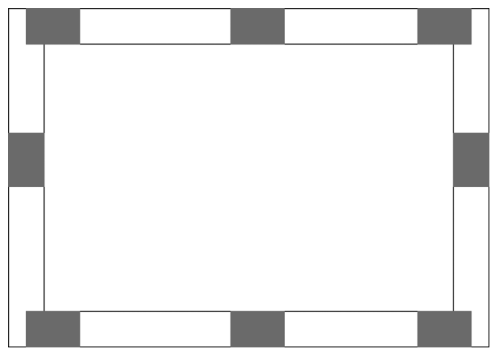

Fig. 2. GUI for brain-actuated control of a wheelchair. Eight flashing buttons are included to evoke P300 potentials.

### B. GUI and Control Mechanism

The GUI, similar to that used in [21] and [22], is illustrated in Fig. 2. A rectangular workspace and eight flashing buttons are included. The workspace is 1166 × 721 pixels. The eight buttons flash in a random order to induce P300 potentials. Each button is intensified for 100 ms, and the time interval between two consecutive button flashes is 120 ms. Thus, one round of button flashes lasts 960 ms (1 round here is defined as a complete cycle in which each button flashes once).

In our system, the subjects are required to control the direction and speed of the simulated or real wheelchair. Two choices, low and high, are available for speed control. To accomplish these control tasks, the BCI system provides the simulated or real wheelchair with the following four commands: turn left, turn right, accelerate and decelerate. As shown in Table I, the user is instructed to implement these commands by performing four tasks to produce these control commands: left-hand motor imagery, right-hand motor imagery, foot motor imagery, and attention to a specific flashing button without motor imagery. If left- or right-hand motor imagery is detected, then the simulated

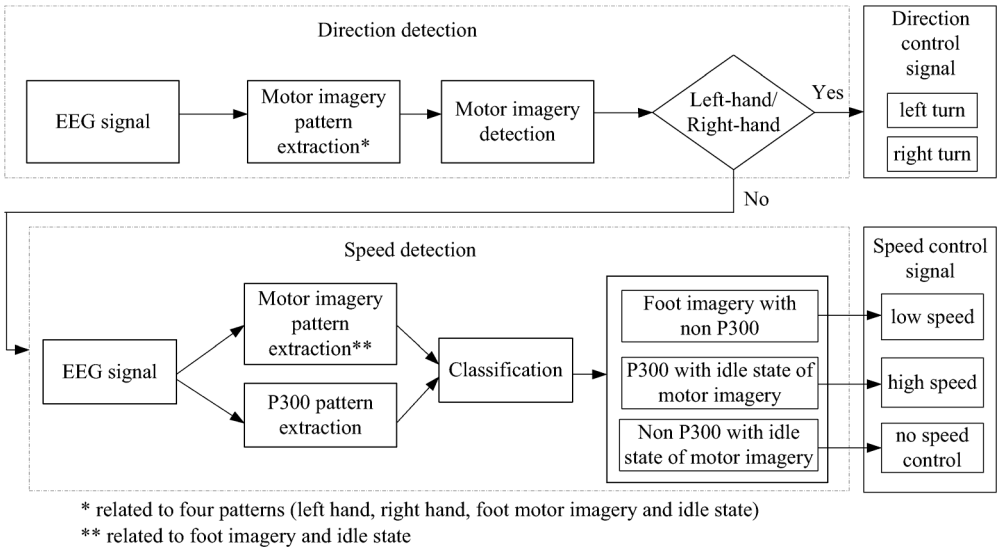


Fig. 3. Diagram for algorithm used in detection of directional and speed control signals. In this paradigm, user imagines left- or right-hand movement to produce a control command for a left or right turn, respectively. To send an deceleration control command, user performs foot motor imagery and ignores flashing buttons. To accelerate, user focuses on a specific button without any motor imagery.

TABLE I
CONTROL COMMANDS AND THEIR CORRESPONDING MENTAL TASKS (MI: MOTOR IMAGERY)

| control commands | mental tasks |
|---|---|
| left turn | left-hand MI |
| right turn | right-hand MI |
| deceleration | foot MI |
| acceleration | focusing on a specific flashing button |
| no control command | idle state |

or real wheelchair turns left or right, respectively. Furthermore, the simulated or real wheelchair does not stop before turning. Separately, the system detects foot movement imagery and the P300 potential for speed control. When a P300 potential with an idle state of motor imagery is detected, the simulated or real wheelchair moves at high speed. By contrast, if foot motor imagery with an idle state of P300 is detected, then the simulated or real wheelchair moves at low speed.

*Remark:* If the P300 modality is not introduced into the BCI system, then one may choose a low speed or high speed by imagining foot movement or remaining idle with regard to motor imagery, respectively. However, the accuracy of idle state detection is often unsatisfactory. Thus, the P300 modality is used in this study.

### C. Models and Algorithms

We propose a hierarchical decision method to steer the simulated or real wheelchair (Fig. 3) by using the directional and speed control commands detected within the user's EEG signals. First, the motor imagery patterns are extracted to identify the directional control commands. If left- or right-hand motor imagery is detected, then it is interpreted as a directional control command for a left or right turn. Otherwise, the speed control commands are extracted. The speed control command for acceleration or deceleration is determined by discriminating the following two tasks executed by the user. The first task is that the user imagines foot movement without attending to a specific flashing button, whereas the other task is that the user pays attention to the specific flashing button without performing any motor imagery. Specifically, if the P300 potential with the idle state of motor imagery is detected, then it is interpreted as an acceleration command; if foot movement imagery with the idle state of P300 is detected, then it is interpreted as a deceleration command; if neither motor imagery nor any P300 potential is detected (the idle state of both motor imagery and P300), then no speed control command is received, and the speed remains unchanged. The algorithms to detect the direction and speed signals are described in the following paragraphs.

*1) Detection of Directional Control Signals:* As described, left- and right-hand motor imagery events are used to turn the simulated or real wheelchair left and right, respectively. One directional control command triggers a fixed, predefined degree of rotation. Two consecutive left or right turn commands lead to a rotation with twice the defined degree of rotation. Hence, the objective in directional control is to detect the left- and right-hand motor imagery within the online EEG signals. The user may be in one of the following five states: left-hand motor imagery, right-hand motor imagery, foot motor imagery, flashing button attention, or idle.

To detect left- or right-hand motor imagery, the EEG signals are first spatially filtered with common average reference (CAR) and then band-pass filtered at 8–32 Hz [24]. Next, we compute spatial patterns using the method of one versus the rest common spatial patterns (OVR-CSP) proposed in [25]. Based on a training dataset collected before online testing, a CSP transformation matrix $(W)$ is calculated for each class against all of the others using the well-known joint diagonalization method [24], [26]. The collection of training data is illustrated in Fig. 4. There are four classes of motor imagery data: left-hand, right-

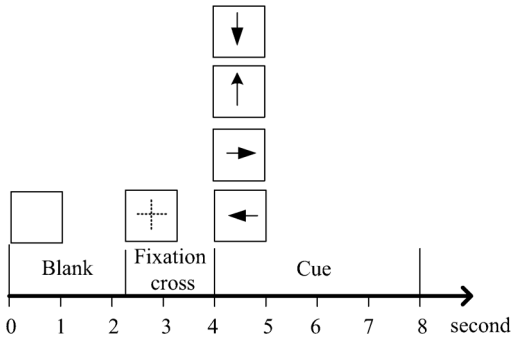


Fig. 4. Paradigm for acquisition of training data in a trial. At the beginning of the trial (0–2.25 s), screen is blank. From 2.25 to 4 s, a cross is shown on screen to capture subject's visual attention. From 4 to 8 s, an arrow cue is shown. Subject is instructed to perform a mental task according to the following cues: left or right arrows cue left- or right-hand motor imagery, up arrow cues foot motor imagery and down arrow cues attention to a specific button (center up button in our experiment). When an arrow appears on screen, eight buttons flash alternately in random order. Brightness of each button intensifies for 100 ms, and time interval between two consecutive button flashes is 120 ms. Thus, one round of button flashes takes 960 ms, and there are four rounds (repeats) of button flashes per trial.

hand, foot and idle state. Thus, we obtain four CSP transformation matrices. The first and last rows of each CSP transformation matrix $(W)$ correspond to a large response in the first and second conditions, respectively. Therefore, the common practice in a classification setting is to use several rows from both ends of the transformation matrix $W$ as spatial filters. If the number of the rows used for spatial filtering is too small, the classifier would fail to fully capture the discrimination between two classes; on the other hand, the classifier weights could severely overfit if the number of the rows is too large [27]. In this study, we select the first and last three rows from each of the four CSP transformation matrices to construct a new transformation matrix with 24 rows for feature extraction following [27].

The logarithmic variances of the projections of the EEG signals from the transformation matrix are used as the features of the signal. Furthermore, the training data set is used to train four linear discriminant analysis (LDA) classifiers with the *one-versus-rest* method for dealing with the multi-class classification problem [28]. For online testing, these four LDA classifiers are applied to the feature vector extracted from the EEG data during the 1000-ms period before the current time point. Hence, four LDA output scores are obtained. Following a loss-based decoding method described in [28], the feature vector is given the class label corresponding to the maximal score. This detection is performed every 200 ms.

The direction of the simulated or real wheelchair's motion will remain constant if the user imagines foot movement or is idle with regard to motor imagery. In this case, the speed control signals are extracted as described in the next section.

*2) Detection of Speed Control Signals:* If no directional control signals are detected, then speed control signals are extracted. Unlike directional control, speed control is implemented by combining two types of EEG patterns: the ERD/ERS of the sensorimotor rhythms and the P300 potential. As described in Section II-B, the speed control signal is detected by discriminating two states: foot motor imagery without button attention and focus on a specific button without motor imagery.

There are two feature extractions for speed detection (Fig. 3): one is for motor imagery detection and the other is for P300 potential detection. First, we describe the feature extraction for motor imagery detection using the training data. Here, the training data set contains two classes of data corresponding to foot motor imagery and the idle state of motor imagery (attention to a specific button). If a trial in the training data corresponds to the idle state of motor imagery, then its label is set to 1. Otherwise, its label is $-1$, corresponding to the foot imagery. A CSP transformation matrix $(W_1)$ is calculated similarly to that described in Section II-C1. Thus, a feature vector $x_j$ for the $j$th trial of the training data can be constructed by projecting the $j$th trial EEG signal on the top and bottom three rows of $W_1$ and then calculating their logarithm variances as the motor imagery features, where $j = 1, \ldots, N$.

The P300 feature extraction for the $j$th trial of the training data $(j = 1, \ldots, N)$ is similar to that described in [29] and [21]. First, the EEG signals are filtered between 0.1 and 20 Hz. Then, we extract a segment (0–600 ms after a button flash) of EEG signals from each channel for each flash of the button (specifically, the center up button in our experiment). The segment is downsampled by a rate of 6 to obtain a data vector from each channel. For each flash of the specific button, a new data vector with 375 dimensions (25 time points $\times 15$ channels) is obtained by concatenating the data vectors from all 15 channels. The feature vector $(p_j)$ in each trial is obtained by averaging four data vectors corresponding to four repeats of the button flash. If the trial in the training data corresponds to attention to the specific button, then the label is set to 1. Otherwise, the label is $-1$.

After extracting the motor imagery feature $x_j$ and the P300 feature $p_j$ $(j = 1, \ldots, N)$ based on the training data set, a combination algorithm, PROB, is used to combine the features of these two modalities [25]. Specifically, two LDA classifiers, denoted as $(w_X, b_X)$ and $(w_P, b_P)$, are trained using the motor imagery feature vectors with labels and the P300 feature vectors with labels, respectively. Two scores for each trial's motor imagery feature vector and P300 feature vector pair are computed using the corresponding classifiers. Next, we calculate the sum of these two scores as

$$D_j = \frac{1}{2}\left[w_X^T x_j + b_X\right] + \frac{1}{2}\left[w_P^T p_j + b_P\right], \quad j = 1, \ldots, N. \tag{1}$$

Using $D_j$, we calculate two thresholds, $D^+_{\text{mean}}$ and $D^-_{\text{mean}}$, as follows:

$$D^+_{\text{mean}} = \frac{1}{|D^+|}\sum_{j \in D^+} D_j$$
$$D^-_{\text{mean}} = \frac{1}{|D^-|}\sum_{j \in D^-} D_j \tag{2}$$

where $D^+$ and $D^-$ denote the set of indices of $D_j$ satisfying $D_j > D_{\text{mean}}$ and $D_j < D_{\text{mean}}$, respectively $(j = 1, \ldots, N)$, $D_{\text{mean}}$ is the mean of all $D_j$, and $|*|$ is the cardinality of a set.

In the test phase, a motor imagery feature vector is extracted every 200 ms using EEG data collected during the 1000-ms period before the current time point, whereas a P300 feature vector is extracted at every flash of the specific button as above. Specifically, the P300 feature extraction is based on the EEG data ac-

quired during four repeats of the button flash (the current flash and the three prior flashes). The speed signal detection is performed every 200 ms based on the motor imagery feature vector updated every 200 ms and the P300 feature vector updated every 960 ms (a complete round of button flashes).

A score denoted as $D$ is then calculated as described in (1). A label $\hat{y}$ for this epoch of EEG data is defined as

$$\hat{y} = \begin{cases} +1, & \text{if } D > D^{+}_{\text{mean}} \\ 0, & \text{if } D^{-}_{\text{mean}} \leq D \leq D^{+}_{\text{mean}} \\ -1, & \text{if } D < D^{-}_{\text{mean}}. \end{cases} \quad (3)$$

In (3), if $\hat{y} = 1$, then the system decides that the user is paying attention to a specific flashing button and is not performing any motor imagery. This case results in an acceleration command. If $\hat{y} = -1$, then the system decides that the user is imagining foot movement and ignoring the flashing buttons. This case results in a deceleration command. If $\hat{y} = 0$, then the user is considered to be idle with regard to both motor imagery and P300 potential; no speed control command is given to the simulated or real wheelchair.

## III. Experimental Results

To validate our proposed hybrid BCI system for detecting directional and speed control commands, two experiments were conducted. The first experiment utilized a simulated wheelchair in a virtual environment, and the second experiment used a real wheelchair.

According to [2], we used the following performance indices to assess our hybrid BCI with respect to directional and speed control.

1) Accuracy rate: the percentage of successful navigation tasks.
2) Path length: the distance (pixels/meters) traveled to accomplish the task.
3) Path length optimality ratio: the ratio of the path length to the optimal path length. The optimal path length is the sum of point-to-point distances between each pair of adjacent destinations.
4) Time: the time $(s)$ to accomplish the task.
5) Time for low speed: the time $(s)$ during which the simulated wheelchair travels at low speed.
6) Wrong speed control time: in the second experiment (real wheelchair), the path for the wheelchair is separated into ten segments; five segments are set for low speed and five are set for high speed. This index represents the time that the wheelchair travels at low speed in the segments designated for high speed and vice versa.
7) Collisions: the number of collisions incurred to the edges of the working space by the simulated wheelchair or to the corridor by the real wheelchair.

### A. Experiment 1: A Simulated Wheelchair Test

In this experiment, we tested whether a user could steer a simulated wheelchair in a virtual environment using the directional and speed controls. The simulated wheelchair and six fixed destinations (circles) are shown in Fig. 5. We defined two routes for each user by setting the order of destinations, and the two routes are presented in Fig. 5(a) and (b). The numbers in these

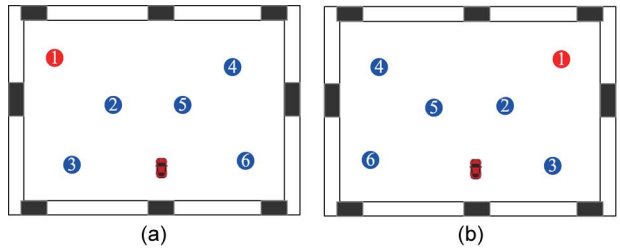


Fig. 5. Simulated wheelchair and two predefined routes.

circles denote the order in which the simulated wheelchair arrives at each destination. Both routes had the same optimal path length of 2270 pixels. The current destination, where the simulated wheelchair was first located, is marked red. When the subject drives the simulated wheelchair through the current destination at low speed, the color of this circle changes to blue and the next circle changes to red. If, however, the simulated wheelchair passes the current destination at high speed, then the circle remains red, and it is considered "missed". The user must drive the simulated wheelchair through the missed circle again (at low speed) until the color changes. The working space and the control task designs originate from the Automatic Car Control event at the BCI competition held in China (2010), which was organized by Tsinghua University. During the competition, the order of the destinations was randomly set for each participant. The hybrid BCI system described here won first place in this competition.

The user GUI and the control mechanism were described in Section II. Five subjects participated in this experiment. There were three sessions for each subject, and each session consisted of ten trials. In each trial, one of the two predefined routes was randomly selected. The subject was required to drive the simulated wheelchair past the six circles sequentially at low speed while trying to proceed as quickly as possible, similar to the requirements of the BCI competition in China (2010). Furthermore, if the user did not accomplish this task within 2 minutes, then the trial was considered a failure and was automatically terminated. In this experiment, the high and low speeds were set to 40 and 20 pixels/s, respectively. The rotational speed was set to 6° per directional control command.

The experimental results are summarized in Table II. All of the subjects accomplished each predefined task successfully using the directional and speed controls for the simulated wheelchair. The average path optimality ratio was 1.25, indicating a difference between the optimal path length and the actual path length taken by the subjects. This difference was mainly due to the extra distance required to turn sharply around each destination; directional correction occurred in the open space. Furthermore, no collisions occurred during the experiment. Thus, the performance of our proposed hybrid BCI system for directional control was satisfactory. In this experiment, the subjects were required to accomplish the tasks as quickly as possible. The average time spent at low speed during the completion of the route in a trial was 26.67 s (our experimental requirements compelled the user to drive the simulated wheelchair through the destinations at a low speed). The average total time to accomplish the tasks during a trial was

TABLE II
PERFORMANCE INDICES FOR ASSESSING SIMULATED WHEELCHAIR DRIVEN BY OUR HYBRID BCI

| | Accuracy rate (%) | Path length ($pixel$) | Path opt. ratio | Time ($s$) | Time for low speed (s) | Collisions |
|---|---|---|---|---|---|---|
| S1 | 100±0 | 2837.35±66.63 | 1.25±0.04 | 82.11±1.62 | 22.35±1.22 | 0±0 |
| S2 | 100±0 | 2761.13±51.26 | 1.22±0.03 | 80.84±1.35 | 23.63±1.45 | 0±0 |
| S3 | 100±0 | 2919.65±76.42 | 1.29±0.03 | 88.39±1.26 | 30.80±1.76 | 0±0 |
| S4 | 100±0 | 2856.32±73.27 | 1.26±0.04 | 85.02±1.19 | 27.22±1.23 | 0±0 |
| S5 | 100±0 | 2842.32±54.71 | 1.25±0.02 | 85.75±1.22 | 29.38±1.15 | 0±0 |
| mean±std | 100±0 | 2843.46±105.41 | 1.25±0.05 | 84.42±4.63 | 26.67±4.18 | 0±0 |

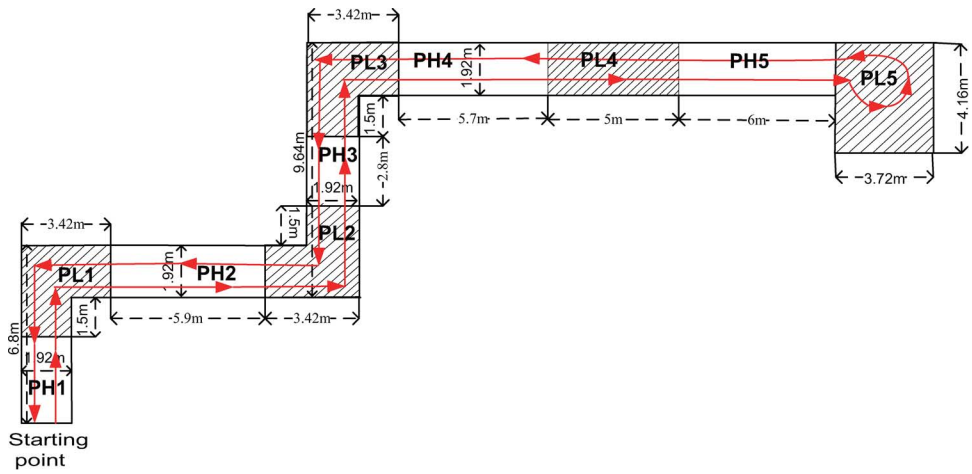


Fig. 6. Top-down view of wheelchair route in second experiment. Shaded parts represent low-speed areas, and unshaded parts represent high-speed areas. Red curve indicates real path of a wheelchair during a trial.

84.42 s. Thus, on average, the simulated wheelchair traveled at high speed for 57.75 s $(84.42 - 26.67 = 57.75$ s) of the trial period. This implies that all subjects performed speed control effectively using our hybrid BCI system.

### B. Experiment 2: Test of a Real Wheelchair

In this experiment, a real wheelchair was controlled using our hybrid BCI. The wheelchair footprint was 0.67 m × 0.9 m, and the ratio of the width of the wheelchair to the width of path was 0.35. Using the user GUI and the control mechanism described in Section II, two subjects (S1 and S2) participated in this experiment, and each subject performed five trials. In each trial, the user was required to drive the wheelchair from a starting point to a goal area following the predefined route shown in Fig. 6. Next, the user was instructed to perform a "U" turn in the goal area and then return to the starting point along the predefined route. Unlike the path in the first experiment, this path was separated into ten segments. The subjects were required to drive the wheelchair past the five shaded parts (PL1–PL5) at low speed and past the other five parts (PH1–PH5) at high speed. Note that PL5 was used as a goal area. In this experiment, the high and low speeds were set to 0.3 and 0.1 m/s, respectively; the rotational speed was set to 10° per directional control command. In a real environment, however, the wheelchair might not turn 10° for each directional control command given because the degree of rotation is affected by several factors including the terrain topography. Thus, if a 90° turn is required, then the user may continuously send directional control commands (one directional control command every 200 ms) until the wheelchair completes the 90° turn. In the experiment shown in Fig. 6, about 2.5 s is required for the wheelchair to turn 90°.

We show the average results of the two subjects for low-speed areas (PL1–PL5) and high-speed areas (PH1–PH5) in Tables III and IV, respectively. For segments PL1–PL5, the wheelchair was required to travel at low speed. The recorded wrong speed control time 4.54 s for a segment of PL1–PL5 (averaged across all these segments) indicates the amount of time that the wheelchair traveled at high speed during this period. Conversely, the recorded wrong speed control time 4.16 s for a segment of PH1–PH5 (averaged across all these segments) indicates the amount of time that the wheelchair traveled at low speed during this period. By comparing the wrong speed control time of 4.54 or 4.16 s with the average time of 45.38 or 20.14 s to cover each segment of PL1–PL5 or PH1–PH5, respectively, we can conclude that the two subjects controlled the speed of the wheelchair effectively. Although the precise path length was difficult to obtain online without sensors, the path lengths of low and high speed segments were approximated offline using the corresponding travel times and speed (low speed or high speed). The average path optimality ratios were 1.14 and 1.1 for low- and high-speed areas, respectively. Note that the path optimality ratio of PL5 is not presented here because the wheelchair performed a "U" turn in this area. No collisions were observed. These results demonstrate that the two subjects successfully drove a wheelchair in the narrow corridor using effective directional control.

TABLE III
PERFORMANCE INDICES (AVERAGED FROM TWO SUBJECTS) OBTAINED WITH REAL WHEELCHAIR IN LOW SPEED AREAS

| | Path length ($m$) | Path opt. ratio | Time ($s$) | Wrong speed control time ($s$) | Collisions |
|---|---|---|---|---|---|
| PL1 | 5.82±0.26 | 1.18±0.02 | 47.72±1.46 | 5.25±0.62 | 0±0 |
| PL2 | 5.68±0.24 | 1.15±0.02 | 49.98±1.65 | 3.50±0.51 | 0±0 |
| PL3 | 5.71±0.21 | 1.16±0.03 | 47.96±1.67 | 4.80±0.76 | 0±0 |
| PL4 | 5.41±0.16 | 1.08±0.02 | 45.99±1.31 | 4.14±0.45 | 0±0 |
| PL5 | 4.52±1.23 | | 35.27±2.13 | 4.94±0.82 | 0±0 |
| mean±std | 5.43±2.02 | 1.14±0.07 | 45.38±5.51 | 4.54±1.24 | 0±0 |

TABLE IV
PERFORMANCE INDICES (AVERAGED FROM TWO SUBJECTS) OBTAINED WITH REAL WHEELCHAIR IN HIGH SPEED AREAS

| | Path length ($m$) | Path opt. ratio | Time ($s$) | Wrong speed control time ($s$) | Collisions |
|---|---|---|---|---|---|
| PH1 | 3.75±0.16 | 1.11±0.02 | 14.75±0.05 | 3.38±0.23 | 0±0 |
| PH2 | 6.37±0.23 | 1.08±0.03 | 24.20±0.04 | 4.45±0.57 | 0±0 |
| PH3 | 3n.14±0.13 | 1.12±0.01 | 12.46±0.06 | 2.99±0.38 | 0±0 |
| PH4 | 6.27±0.18 | 1.10±0.02 | 24.24±0.06 | 5.01±0.52 | 0±0 |
| PH5 | 6.54±0.15 | 1.09±0.02 | 25.07±0.07 | 4.91±0.64 | 0±0 |
| mean±std | 5.21±1.54 | 1.10±0.04 | 20.14±6.27 | 4.16±1.36 | 0±0 |

## IV. DISCUSSION

In this paper, we introduce a hybrid BCI to control a simulated or real wheelchair. The benefits of using two control modalities (motor imagery and the P300 potential) include the availability of more commands to allow continuous control and the improvement of control classification accuracy. To demonstrate these benefits, we analyzed the training data collected in the first experiment, which were used to set the parameters of the simulated wheelchair. A nine-fold cross validation was performed for each subject. The results revealed that for five subjects, the average classification accuracy rate ($\mathrm{ACC_{MI}}$) in discriminating between foot imagery and no motor imagery was 71.68 ± 2.41%; the average classification accuracy rate ($\mathrm{ACC}_{P300}$) between P300 potential and no P300 evoked was 80.44 ± 1.82%; and the average classification accuracy rate ($\mathrm{ACC_{hybrid}}$) between foot imagery without P300 potential and P300 potential evoked without motor imagery was 83.10 ± 2.12%. Paired t-tests demonstrated that the $\mathrm{ACC_{hybrid}}$ was significantly higher than the $\mathrm{ACC_{MI}}$ ($t(4) = 32.69, p < 0.001$) and the $\mathrm{ACC}_{P300}$ ($t(4) = 18.24, p < 0.001$). Fig. 7 shows the three average receiver operator characteristic (ROC) curves for all subjects; i.e., the black, cyan, and magenta ROC curves correspond to the classification between foot imagery and no motor imagery, the classification between P300 potential and no P300 potential evoked, and the classification between foot imagery without P300 potential signal and P300 potential evoked without motor imagery (hybrid), respectively. As shown in Fig. 7, the area under the magenta ROC curve is the largest among the three ROC curves.

To clearly demonstrate the control procedure, the trajectories corresponding to two routes obtained from two trials of experiment 1 for subject S1 are presented in Fig. 8. In these trajectories, the red- and black-colored sections represent the high- and low-speed portions, respectively. Thus, the direction and speed of the simulated wheelchair can be effectively controlled using our hybrid BCI.

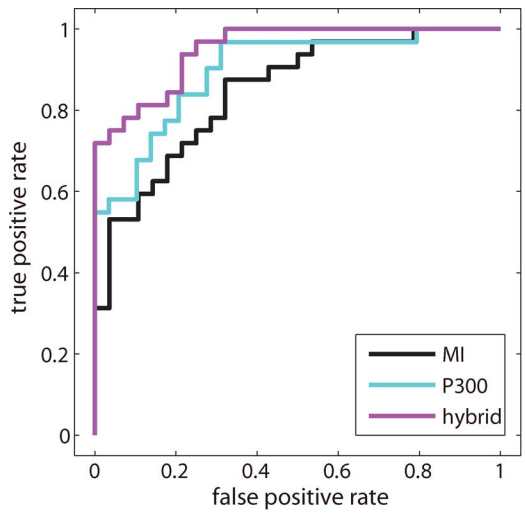


Fig. 7. Three average ROC curves across all subjects corresponding to three classifications: between foot motor imagery and idle state of motor imagery (MI), between P300 potential and no P300 potential (P300), between foot motor imagery without P300 potential and P300 potential without motor imagery (hybrid).

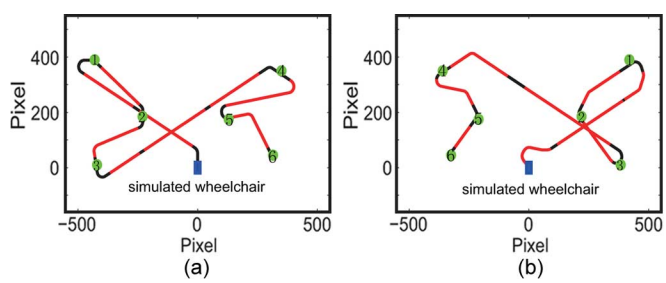


Fig. 8. Two trajectories corresponding to two routes traveled by subject S1 in the first experiment. Red and black indicate high and low speed, respectively.

To use our hybrid BCI control strategy, the user is required to focus on a flashing button to accelerate the simulated or real

wheelchair. Simultaneously, the subject must focus on the route and state of movement. Our experience shows that it is not difficult for an experienced user to perform these two tasks simultaneously because acceleration often occurs where there is sufficient space for the simulated or real wheelchair.

In our previous study [22], a hybrid BCI that combines motor imagery and the P300 potential was used for cursor control and target selection. Specifically, the user paid attention to a specific flashing button without performing any motor imagery to select a target. By contrast, he/she performed left-hand or right-hand motor imagery with no attention to the specific flashing button to reject a target. It was demonstrated that this hybrid control strategy using the two modalities has better discriminating performance than that based on a single modality of the motor imagery or the P300 potential. The feasibility and advantages of hybrid BCIs have also been demonstrated by other studies, e.g., [20] and [23]. In this work, a similar hybrid strategy employing foot motor imagery and the P300 potential is used to control speed (acceleration/deceleration) of a wheelchair, and its efficacy was demonstrated by our experiments.

Furthermore, it is important to have a stop command in the BCI control system of a real wheelchair. However, it is difficult to design an effective (fast and accurate) stop command. To our knowledge, only one study [3] utilized a stop command. In [3], the user first selected a destination among a list of predefined locations using a slow but reliable P300-based BCI, and the wheelchair automatically moved on a virtual guiding path. The user could stop the wheelchair in an average 6 or 4.9 s by using a faster P300- or motor imagery-based BCI. Currently, we are exploring the possibility of combining the SSVEP with electromyography (EMG) to produce a fast and accurate stop command in our system. For instance, its execution time should be significantly faster than the benchmark in [3]. We will report our results in future work.

In this study, the four-class classification is related to left-hand, right-hand and foot motor imagery tasks and the idle state of motor imagery. However, during periods not performing motor imagery, the user may pay attention to a specific flashing button to evoke a P300 potential. The following analysis indicates that adding the option to evoke a P300 potential will not affect the performance of motor imagery in terms of the classification accuracy.

First, although the entire frequency band (0.1–20 Hz) is used to extract P300 features in this study, the P300 potential is mainly in the low-frequency band below 8 Hz [30], whereas the ERD/ERS related to motor imagery occurs in the mu/beta rhythm with a frequency exceeding 8 Hz. This is also demonstrated in Fig. 9, in which the first subplot shows the ERP curves calculated from the training EEG data in the frequency band of 0.1–8 Hz, and the second shows the ERP curves based on the same EEG data but in the frequency band of 8–32 Hz.

Furthermore, we collected two experimental datasets. Each of the two datasets includes four classes of trials including 30 trials of left-hand motor imagery, 30 trials of right-hand motor imagery, 30 trials of foot motor imagery, and either 30 trials of attention to a specific flashing button without motor imagery in the first dataset or 30 trials of the idle state (no button attention and no motor imagery) in the second data set. The time course

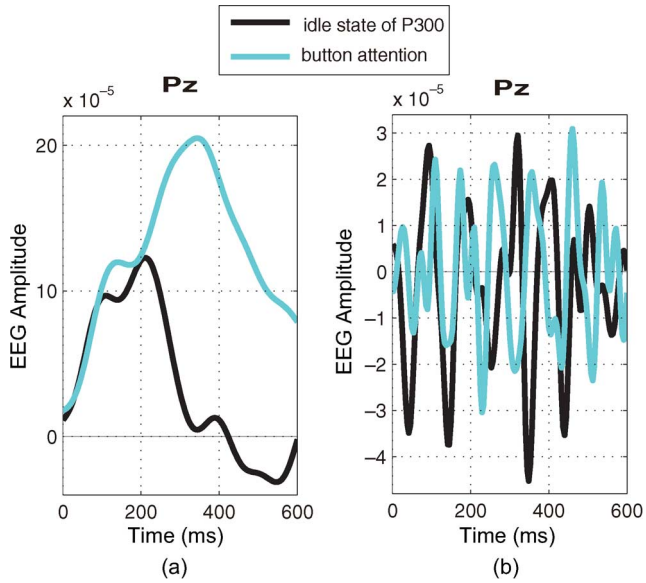


Fig. 9. (A) Two ERP curves for Subject 1, calculated from EEG signal of channel Pz filtered with frequency band of 0.1–8 Hz; cyan curve corresponding to button attention contains evoked P300 potential, whereas black curve corresponding to idle state of button attention does not contain evoked P300 potential. (B) Two ERP curves for Subject 1, calculated from EEG signal of channel Pz filtered with frequency band of 8–32 Hz; neither of the curves, corresponding to button attention and the idle state of button attention, respectively, contains P300 potential.

TABLE V
FOUR-CLASS CLASSIFICATION ACCURACY RATES FOR TWO DATASETS COLLECTED FROM HYBRID-TASK EXPERIMENT AND MOTOR IMAGERY (MI)-TASK EXPERIMENT

| subjects | Hybrid-task accuracy (%) | MI-task accuracy (%) |
|---|---|---|
| S1 | 75.6± 1.7 | 76.5 ± 1.8 |
| S2 | 76.3± 1.9 | 74.6 ± 1.7 |
| S3 | 74.2± 1.6 | 75.8 ± 2.2 |
| S4 | 77.1± 2.1 | 76.4 ± 1.6 |
| S5 | 73.8± 1.2 | 74.8 ± 1.1 |
| mean± std | 75.4± 1.4 | 75.6 ± 0.9 |

of each trial is the same as that in Fig. 4, and the order of all of the trials in each dataset is random. Table V shows the accuracy rates of our four-class classification, obtained through a ten-fold cross validation of each of the two datasets. No significant difference is found between the accuracy rates for the first dataset concerning hybrid tasks and those for the second dataset concerning only motor imagery tasks ($p = 0.86$, paired Students t-test). The results here also demonstrated that adding the P300 task will not affect the performance of motor imagery and, thus, does not affect the classification accuracy.

Finally, as described in Section II-C1, our four-class classification concerning left-hand, right-hand and foot motor imagery and the idle state of motor imagery is performed through four one-versus-rest classifiers. For each classifier, we train a OVR-CSP transformation matrix for feature extraction. Fig. 10 shows the topographies of the four selected CSP filters (the first row of each OVR-CSP transformation matrix), obtained using the training dataset of subject 1. Although the user pays attention to a specific flashing button during the idle state of motor imagery, the topographies of the CSP filters in Fig. 10 exhibit

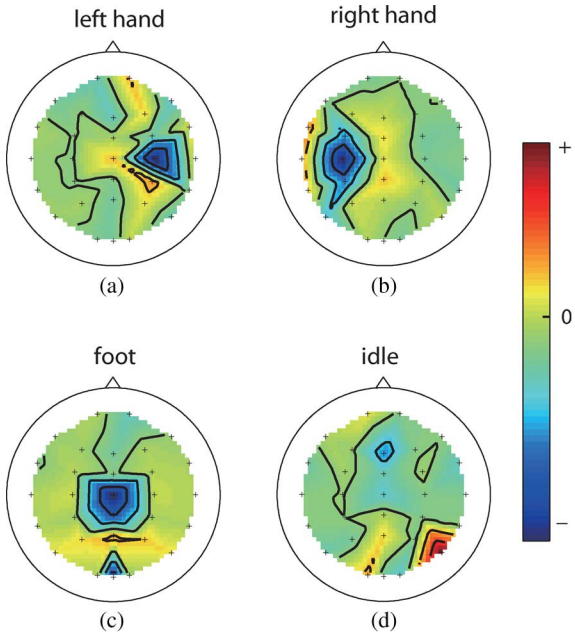


Fig. 10. Scalp maps of CSP weights for subject 1. (A) Scalp map of the first row of OVR-CSP transformation matrix to discriminate between left-hand motor imagery and the other three mental states. (B) Scalp map of the first row of OVR-CSP transformation matrix to discriminate between right-hand motor imagery and the other three mental states. (C) Scalp map of the first row of OVR-CSP transformation matrix to discriminate between foot motor imagery and other three mental states. (D) Scalp map of the first row of OVR-CSP transformation matrix to discriminate between idle state and the other three mental states.

the brain patterns related to motor imagery, which are similar to those reported in existing studies (e.g., [31]) that involve only the three types of motor imagery.

## V. Conclusion

This paper presents a hybrid BCI that combines the mu/beta rhythm resulting from motor imagery and the P300 potential for the directional and speed control of a simulated or real wheelchair. Four commands are each associated with a mental task. Specifically, the user performs left- or right-hand motor imagery to direct a left or right movement and performs foot imagery or focuses on a flashing button to adjust the speed of the simulated or real wheelchair. Two experiments were conducted. One used a simulated wheelchair in a virtual environment, and the other utilized a real wheelchair. Both experiments demonstrated the effectiveness of our method and system. Further data analysis indicated that the use of multiple signal modalities (motor imagery and P300 potentials) is useful not only to provide multiple independent control signals but also to improve accuracy (classification performance). In our future work, we will implement additional control signals to this hybrid BCI system for wheelchair control.

## References

[1] J. R. Millán, R. Rupp, G. R. Müller-Putz, R. Murray-Smith, C. Giugliemma, M. Tangermann, C. Vidaurre, F. Cincotti, A. Kübler, R. Leeb, C. Neuper, K.-R. Müller, and D. Mattia, "Combining brain-computer interfaces and assistive technologies: State-of-the-art and challenges," *Front. Neurosci.*, vol. 4, pp. 1–15, 2010.

[2] I. Iturrate, J. M. Antelis, A. Kubler, and J. Minguez, "A noninvasive brain-actuated wheelchair based on a p300 neurophysiological protocol and automated navigation," *IEEE Trans. Robot.*, vol. 25, no. 3, pp. 614–627, Mar. 2009.

[3] B. Rebsamen, C. Guan, H. Zhang, C. Wang, C. Teo, M. H. Ang, and E. Burdet, "A brain controlled wheelchair to navigate in familiar environments," *IEEE Trans. Neural Syst. Rehab. Eng.*, vol. 18, no. 6, pp. 590–598, Jun. 2010.

[4] F. Galán, M. Nuttin, E. Lew, P. W. Ferrez, G. Vanacker, J. Philips, and J. R. Millán, "A brain-actuated wheelchair: Asynchronous and non-invasive Brain-computer interfaces for continuous control of robots," *Clin. Neurophysiol.*, vol. 119, no. 9, pp. 2159–2169, 2008.

[5] K. Tanaka, K. Matsunaga, and H. O. Wang, "Electroencephalogram-based control of an electric wheelchair," *IEEE Trans. Robot.*, vol. 21, no. 4, pp. 762–766, Apr. 2005.

[6] L. A. Farwell and E. Donchin, "Talking off the top of your head: Toward a mental prosthesis utilizing event-related brain potentials," *Electroencephalogr. Clin. Neurophysiol.*, vol. 70, no. 6, pp. 510–523, 1988.

[7] M. Middendorf, G. McMillan, G. Calhoun, and K. S. Jones, "Brain-computer interfaces based on the steady-state visual-evoked response," *IEEE Trans. Neural Syst. Rehab. Eng.*, vol. 8, no. 2, pp. 211–214, Feb. 2000.

[8] G. R. Müller-Putz, R. Scherer, C. Neuper, and G. Pfurtscheller, "Steady-state somatosensory evoked potentials: Suitable brain signals for brain-computer interfaces?," *IEEE Trans. Neural Syst. Rehab. Eng.*, vol. 14, no. 1, pp. 30–37, Jan. 2006.

[9] G. Pfurtscheller and F. H. Lopes da Silva, "Event-related EEG/MEG synchronization and desynchronization: Basic principles," *Clin. Neurophysiol.*, vol. 110, no. 11, pp. 1842–1857, 1999.

[10] T. Luth, D. Ojdanic, O. Friman, O. Prenzel, and A. Graser, "Low level control in a semi-autonomous rehabilitation robotic system via a brain-computer interface," in *Proc. IEEE 10th Int. Conf. Rehabil. Robot.*, 2007, pp. 721–728.

[11] J. R. Millán, F. Renkens, J. Mouriño, and W. Gerstner, "Noninvasive brain-actuated control of a mobile robot by human eeg," *IEEE Trans. Biomed. Eng.*, vol. 51, no. 6, pp. 1026–1033, Jun. 2004.

[12] R. Scherer, F. Lee, A. Schlögl, R. Leeb, H. Bischof, and G. Pfurtscheller, "Toward self-paced brain-computer communication: Navigation through virtual worlds," *IEEE Trans. Biomed. Eng.*, vol. 55, no. 2, pp. 675–682, Feb. 2008.

[13] J. R. Wolpaw and D. J. McFarland, "Control of a two-dimensional movement signal by a noninvasive brain-computer interface in humans," *Proc. Nat. Acad. Sci.*, vol. 101, no. 51, pp. 17 849–17 854, 2004.

[14] D. J. McFarland, W. A. Sarnacki, and J. R. Wolpaw, "Electroencephalographic (EEG) control of three-dimensional movement," *J. Neural Eng.*, vol. 7, p. 036007, 2010.

[15] D. J. McFarland, D. J. Krusienski, W. A. Sarnacki, and J. R. Wolpaw, "Emulation of computer mouse control with a noninvasive brain-computer interface," *J. Neural Eng.*, vol. 5, no. 2, pp. 101–110, 2008.

[16] A. S. Royer, A. J. Doud, M. L. Rose, and B. He, "EEG control of a virtual helicopter in 3-dimensional space using intelligent control strategies," *IEEE Trans. Neural Syst. Rehab. Eng.*, vol. 18, no. 6, pp. 581–589, Jun. 2010.

[17] A. J. Doud, J. P. Lucas, M. T. Pisansky, and B. He, "Continuous three-dimensional control of a virtual helicopter using a motor imagery based brain-computer interface," *PLoS ONE*, vol. 6, no. 10, p. e26 322, 2011, 10.1371/journal.pone.0 026 322.

[18] G. Pfurtscheller, B. Z. Allison, C. Brunner, G. Bauernfeind, T. Solis-Escalante, R. Scherer, T. O. Zander, G. R. Müller-Putz, C. Neuper, and N. Birbaumer, "The hybrid BCI," *Front. Neurosci.*, vol. 4, pp. 1–11, 2010.

[19] G. Pfurtscheller, T. Solis-Escalante, R. Ortner, P. Linortner, and G. R. Müller-Putz, "Self-paced operation of an SSVEP-based orthosis with and without an imagery-based brain switch: A feasibility study towards a hybrid BCI," *IEEE Trans. Neural Syst. Rehab. Eng.*, vol. 18, no. 4, pp. 409–414, Apr. 2010.

[20] B. Z. Allison, C. Brunner, V. Kaiser, G. R. Müller-Putz, C. Neuper, and G. Pfurtscheller, "Toward a hybrid brain-computer interface based on imagined movement and visual attention," *J. Neural Eng.*, vol. 7, no. 2, 2010.

[21] Y. Li, J. Long, T. Yu, Z. Yu, C. Wang, H. Zhang, and C. Guan, "An EEG-based BCI system for 2-D cursor control by combining Mu/Beta rhythm and P300 potential," *IEEE Trans. Biomed. Eng.*, vol. 57, no. 10, pp. 2495–2505, Oct. 2010.
[22] J. Long, Y. Li, T. Yu, and Z. Gu, "Target selection with hybrid feature for BCI-based 2-D cursor control," *IEEE Trans. Biomed. Eng.*, to be published.
[23] C. Brunner, B. Z. Allison, D. J. Krusienski, V. Kaiser, G. R. Müller-Putz, G. Pfurtscheller, and C. Neuper, "Improved signal processing approaches in an offline simulation of a hybrid brain-computer interface," *J. Neurosci. Methods*, vol. 188, no. 1, pp. 165–173, 2010.
[24] G. Blanchard and B. Blankertz, "BCI competition 2003-data set IIa: Spatial patterns of self-controlled brain rhythm modulations," *IEEE Trans. Biomed. Eng.*, vol. 51, no. 6, pp. 1062–1066, Jun. 2004.
[25] G. Dornhege, B. Blankertz, G. Curio, and K. R. Müller, "Boosting bit rates in noninvasive EEG single-trial classifications by feature combination and multiclass paradigms," *IEEE Trans. Biomed. Eng.*, vol. 51, no. 6, pp. 993–1002, Jun. 2004.
[26] Y. Li and C. Guan, "Joint feature re-extraction and classification using an iterative semi-supervised support vector machine algorithm," *Mach. Learn.*, vol. 71, no. 1, pp. 33–53, 2008.
[27] B. Blankertz, R. Tomioka, S. Lemm, M. Kawanabe, and K.-R. Müller, "Optimizing spatial filters for robust EEG single-trial analysis," *IEEE Signal Process. Mag.*, vol. 25, no. 1, pp. 41–56, 2008.
[28] E. L. Allwein, R. E. Schapire, and Y. Singer, "Reducing multiclass to binary: A unifying approach for margin classifiers," *J. Mach. Learn. Res.*, vol. 1, pp. 113–141, 2001.
[29] D. J. Krusienski, E. W. Sellers, D. J. McFarland, T. M. Vaughan, and J. R. Wolpaw, "Toward enhanced P300 speller performance," *J. Neurosci. Methods*, vol. 167, no. 1, pp. 15–21, 2008.
[30] H. Serby, E. Yom-Tov, and G. Inbar, "An improved P300-based brain-computer interface," *IEEE Trans. Neural Syst. Rehabil. Eng.*, vol. 13, no. 1, pp. 89–98, Jan. 2005.
[31] G. Pfurtscheller, C. Brunner, A. Schlögl, and F. Lopes da Silva, "Mu rhythm (de) synchronization and EEG single-trial classification of different motor imagery tasks," *Neuroimage*, vol. 31, no. 1, pp. 153–159, 2006.

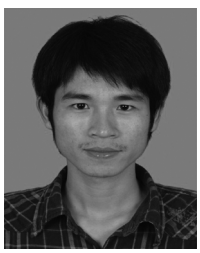

**Jinyi Long** received the B.S. degree in materials processing and controlling engineering from Northeastern University, Shenyang, China, in 2006. He is currently working toward the Ph.D. degree in pattern recognition and intelligent systems, South China University of Technology, Guangzhou, China.

His research interests include machine learning, brain–computer interface, EEG and fMRI data analysis.

**Yuanqing Li** was born in Hunan Province, China, in 1966. He received the B.S. degree in applied mathematics from Wuhan University, Wuhan, China, in 1988, the M.S. degree in applied mathematics from South China Normal University, Guangzhou, China, in 1994, and the Ph.D. degree in control theory and applications from South China University of Technology, Guangzhou, China, in 1997.

Since 1997, he has been with South China University of Technology, where he became a full Professor in 2004. In 2002 through 2004, he worked at the Laboratory for Advanced Brain Signal Processing, RIKEN Brain Science Institute, Saitama, Japan, as a Researcher. In 2004 through 2008, he worked at the Laboratory for Neural Signal Processing, Institute for Infocomm Research, Singapore, as a Research Scientist. His research interests include blind signal processing, sparse representation, machine learning, brain-computer interface, EEG and fMRI data analysis. He is the author or coauthor of more than 60 scientific papers in journals and conference proceedings.

**Hongtao Wang** received the B.S. degree in automatic control from Guangxi University of Technology, Liuzhou, China, in 2004, the M.S. degree in control theory and control engineering from Wuhan University of Technology, Wuhan, China, in 2007. Since 2009, he has been working toward the Ph.D. degree in pattern recognition and intelligent systems at the South China University of Technology, Guangzhou, China.

Since 2007, he has been with School of Information Engineering, WuYi University of Technology as a Lecturer. His research interests include brain–computer interface, pattern recognition and signal processing.

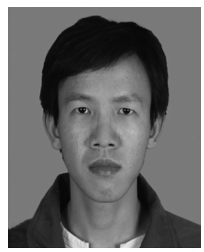

**Tianyou Yu** received the B.Sc. degree in automatic control from the Wuhan University of Science and Technology, Wuhan, China, in 2008. He is currently working toward the Ph.D. degree in pattern recognition and intelligent systems at the South China University of Technology, Guangzhou, China.

His research interests include noninvasive brain-computer interfaces and brain signal analysis.

**Jiahui Pan** received the B.S. degree in computer science and technology from South China Normal University, Guangzhou, China, in 2005, and the M.S. degree in computer application technology from South China Normal University, Guangzhou, China, in 2008. He is currently working toward the Ph.D. degree in pattern recognition and intelligent systems, South China University of Technology, Guangzhou, China.

His research interests include brain–computer interface and medical image processing.

**Feng Li** was born in China in September 1964. He received the B.S. degree in mathematics from Hunan Normal University, China, in 1984, the M.S. degree in computing science from Zhejiang University, China, in 1988, and the Ph.D. degree in computing science from Sun Yat-sen University, China, in 2003.

He is currently a Professor in the School of Computer and Communication Engineering, Changsha University of Science and Technology, China. His research interests include image processing, pattern recognition, information security.